# TRANSACTIONS ON ELECTROMAGNETIC SPECTRUM

# Metasurface-based MIMO Antenna Design and Analysis for 5G Communication Systems

**Ahmet YUMUŞAK[1*]** , **Kayhan ÇELİK[1]**

[1] Department of Electrical and Electronics Engineering, Technology Faculty, Gazi University, Ankara, Türkiye
E-mail:yumusakahmet@yandex.com, kayhancelik1923@gmail.com, kayhancelik@gazi.edu.tr

**\* Corresponding author's e-mail address:** yumusakahmet@yandex.com

**Abstract:** This letter presents a novel four-port multiple-input output (MIMO) antenna incorporating a metasurface (MS) which has been designed for Sub-6 GHz 5G systems. In the design of the MIMO antenna and MS, an FR4 substrate with a thickness of 1.6 mm, a dielectric constant of 4.4, and a loss tangent of 0.02 was used as the dielectric material. The dimensions of the proposed MIMO antenna array are $1.03\ \lambda_0 \times 1.03\ \lambda_0 \times 0.017\ \lambda_0$ at 3.19 GHz, where $\lambda_0$ is the free space wavelength. The proposed metasurface-based antenna operates within the frequency range of 3.19 to 4.06 GHz, effectively covering N78 (3.3-3.8 GHz) 5G band. In addition to the N78 band, it also covers 93.33% of the N77 band (3.3-4.2 GHz). The design achieves an inter-element isolation of more than 17 dB, despite the antenna elements being about $0.34\ \lambda_0$ apart. Furthermore, the metasurface-based MIMO antenna achieves a peak gain of 6.85 dBi, has an ECC value with a maximum value of 0.025, and a DG value of approximately 9.99 dB. As a result, it can be said that the proposed novel antenna structure can be used in various Sub-6 GHz 5G applications.

## 1. INTRODUCTION

The swift rise in the quantity of people utilizing wireless communication technology has caused fifth-generation (5G) communication technologies to be developed to meet demands such as high data transmission rates and low latency [1]. To address these demands, 5G technology introduces requirements for antennas to operate over wide bandwidths, exhibit strong directivity, maintain high inter-port isolation, and provide significant gain [2]. Because of their exceptional adaptability, dependable wide coverage, and ease of integration with other systems, 5G(NR) bands of N77, N78, and N79 are the most widely used in many nations for launching 5G communications [3]. Numerous high-speed, small, smart systems can be integrated with 5G to provide dependable, cutting-edge communications. By increasing channel capacity and reducing multipath fading, the preferred multiple-input multiple-output (MIMO) antenna approach is an optimal strategy to boost spectrum efficiency and reliability in 5G technology. Compared to a single antenna, a MIMO antenna uses multipath propagation to simultaneously deliver incredibly rapid data transmission and reception. By

employing several antennas, the MIMO technique increases the channel capacity to accomplish multipath propagation. MIMO systems were addressed by next-generation communication systems as a workable solution to the data rate issues with single-input single-output (SISO) systems. Consequently, MIMO-type antenna systems are essential for boosting the capacity of the communication system. A MIMO system can accommodate ultra-high data traffic, better capacity, and reliability by using more antenna elements to provide more channels. It can be difficult to build and integrate multiple antennas in a small MIMO system because of the continually rising demand for small, frequency-flexible, and high transmission rate 5G smart devices. MIMO communication capacity and antenna performance are eventually negatively impacted by the significant coupling between antennas brought on by the near proximity of MIMO components. Therefore, one of the most important challenges in compact MIMO technology is to mitigate the coupling impact among the nearby antenna parts. Two essential components of the next 5G communications are the expansion of the bandwidth and downsizing of the antenna volume. To update the MIMO antenna elements in the constrained space with a high-performance antenna, a small and straightforward antenna geometry is ideal. Consequently, a common research trend in the expanding field of high-speed communications is the creation of effective downsized wideband massive MIMO antennas that may be used in the 5G Sub-6 GHz spectrum. To accomplish these and improve performance, numerous methods have been put out in the literature. Some of the methods used to enhance the performance of low-profile microstrip MIMO antennas include decoupling networks (DN), parasitic elements, defected ground structures (DGS), neutralization lines (NL),  the use of metamaterials, and frequency-selective surface (FSS) [4-8]. Some articles in the literature are mentioned. To achieve downsizing and improve the antenna's general effectiveness, two distinct metamaterial structures are created and used by Hasan et al. [3]. Yu, et al. [9] placed a three-dimensional parasitic metamaterial structure between the antenna elements and successfully reduced mutual coupling within the MIMO antenna. Zeain et al. employed a metasurface structure combined with parasitic materials and an FSS to improve both directivity and bandwidth at the Chair-shaped MIMO antenna [10]. Bai et al. introduce a metasurface radiator consisting of nonuniform patches for enhancing gain [11].

Tran et al. [12] achieved high isolation by integrating a metasurface into their antenna design, and metallic vias are used to ground each MIMO element's MS in order to suppress mutual coupling. Din et al. increased the gain of the MIMO array by using an FSS composed of a $7 \times 7$ array with rectangular C-shaped resonators [13]. Square-ring slot antennas fed by the microstrip lines are presented by  Parchin et al. for dual-polarized 5G MIMO applications [14]. Narayanaswamy et al. enhanced the isolation of a DGS-based pentagonal antenna by integrating an absorbing metasurface [15]. Kiem et al. presented a novel circular-shaped UWB antenna with rejected WLAN band using the electromagnetic bandgap [16]. Wong et al. reduced the mutual coupling between antennas using L-shaped metallic walls [17].

A four-port MIMO antenna with a metasurface incorporated has been designed for the purpose of this study to cover the N78 band (3.3–3.8 GHz) and N77 band (3.3-4.2 GHz), which have been allocated for 5G mobile communication systems in many countries worldwide, including Türkiye.

## 2. METASURFACE-BASED MICROSTRIP PATCH ANTENNA DESIGN

In this part of the paper, the designed antenna is explained in detail.  Firstly, the antenna in Fig. 1(a) is designed with the help of Eqs. (1-5). W, L, and $L_{eff}$ represent the antenna's width, length, and effective length. $f_r$ is the antenna's minimum resonation frequency, $h$ is the dielectric material's thickness, and $\varepsilon_r$ and $\varepsilon_{eff}$, stand for the material's relative and effective dielectric constants due to fringing effects [18, 19].

$$W = \frac{c}{2f_r}\sqrt{\frac{2}{\varepsilon_r + 1}} \tag{1}$$

$$\varepsilon_{eff} = \frac{\varepsilon_r+1}{2} + \frac{\varepsilon_r-1}{2}[1 + 12\frac{h}{W}]^{-\frac{1}{2}} \tag{2}$$

$$\Delta L = 0.412h\frac{(\varepsilon_{eff} + 0.3)(\frac{W}{h} + 0.264)}{(\varepsilon_{eff} - 0.258)(\frac{W}{h} + 0.8)} \tag{3}$$

$$L = L_{eff} - 2\Delta L \tag{4}$$

$$L_{eff} = \frac{c}{2fr\sqrt{\varepsilon_{eff}}} \tag{5}$$

The lower part of this antenna consists of a ground plane, and the upper part consists of a radiating patch. Between them there is a 1.6 mm-thick FR4 material with a dielectric constant of 4.4 and a loss tangent of 0.02. In the second step, the same dielectric material is placed on top of this antenna, and square patches with grid-shaped cavities (metasurface) are placed on top of it, as in Fig. 1(b). In the third step, a semicircular slot is added inside the patch to improve antenna performance, as in Fig. 1(c). All the parameters of the antenna are illustrated in Fig. 2(a) and given in Table 1. A coaxial feed powers the antenna, which is apparent in Fig. 2(b). The ANSYS-HFSS simulation program is used in this work to design the antenna and metasurface.
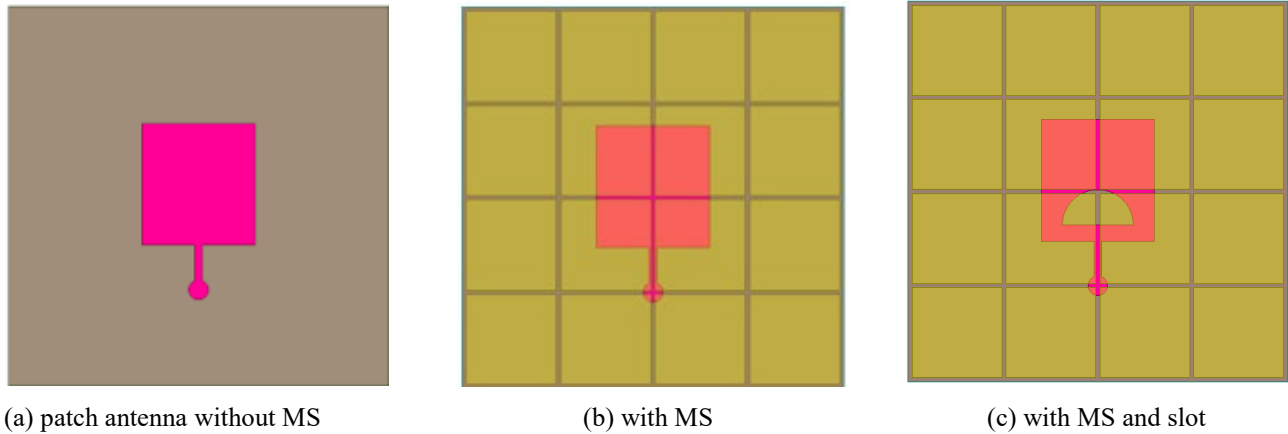
| (a) patch antenna without MS | (b) with MS | (c) with MS and slot |

**Figure 1.** The antenna's planned geometry

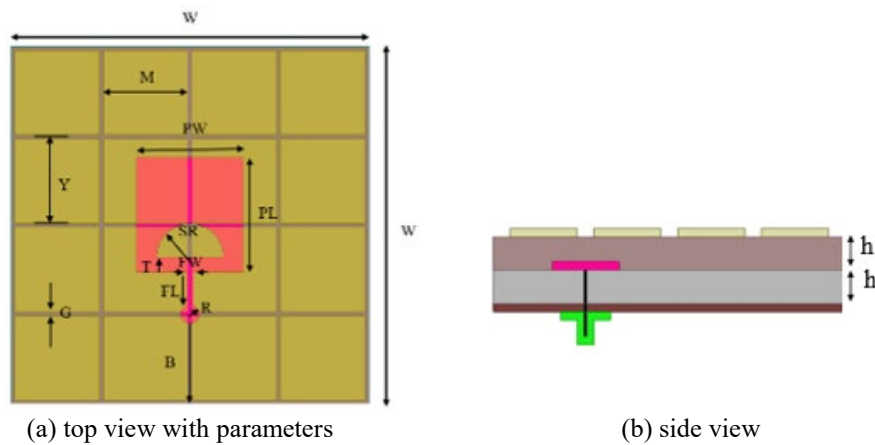| (a) top view with parameters | (b) side view |

**Figure 2.** The antenna layout with parameters and side view

**Table 1**. Design details of single antenna parameters

| Parameter | Size (mm) | Parameter | Size (mm) |
|-----------|-----------|-----------|-----------|
| W | 48.5 | SR | 4.55 |
| PW | 14.5 | B | 11.15 |
| PL | 15.5 | G | 0.54 |
| FL | 4.55 | M | 11.45 |
| R | 1.25 | Y | 11.99 |
| FW | 1 | h | 1.6 |
| T | 2 | Total size | 48.5 x 48.5 x 3.2 |

The reflection coefficients of the microstrip patch antenna in different configurations are presented in Fig. 3. Both the slotted and non-slotted antennas do not resonate in the absence of the MS. When the MS is added to the non-slotted antenna, resonance occurs in the 3.20–3.41 GHz band. It has been noted that introducing a slot on the patch along with the addition of the MS increases the antenna's bandwidth, resulting in resonance over the 3.23–4.13 GHz band.
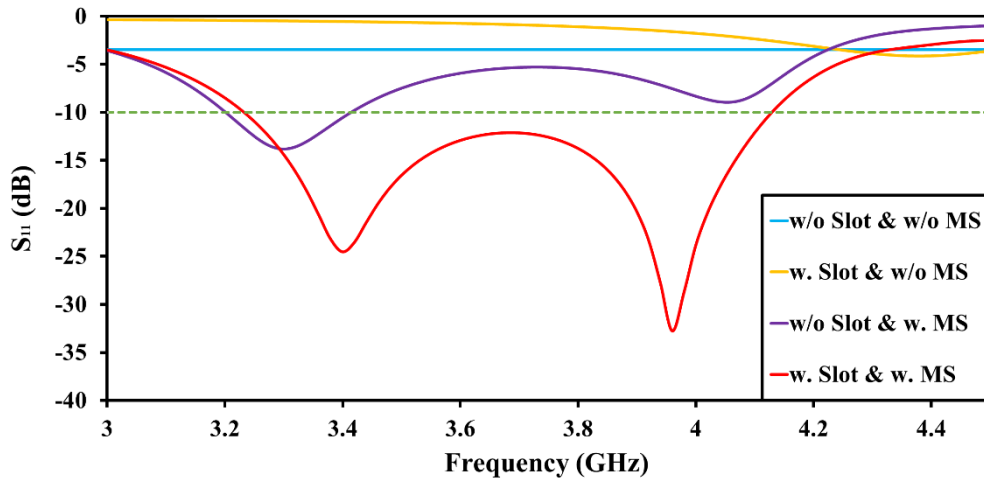


**Figure 3.** Microstrip patch antennas' reflection coefficient with and without slot and MS

## 3. METASURFACE-BASED MICROSTRIP MIMO ANTENNA DESIGN

Fig. 4 depicts the setup of the suggested MIMO antenna. It consists of four microstrip patch antennas with coaxial feeding, sharing a common ground plane. A metasurface structure referred to as an MS, composed of two-dimensional metallic plates, is positioned without an air gap directly on top of the MIMO antenna.
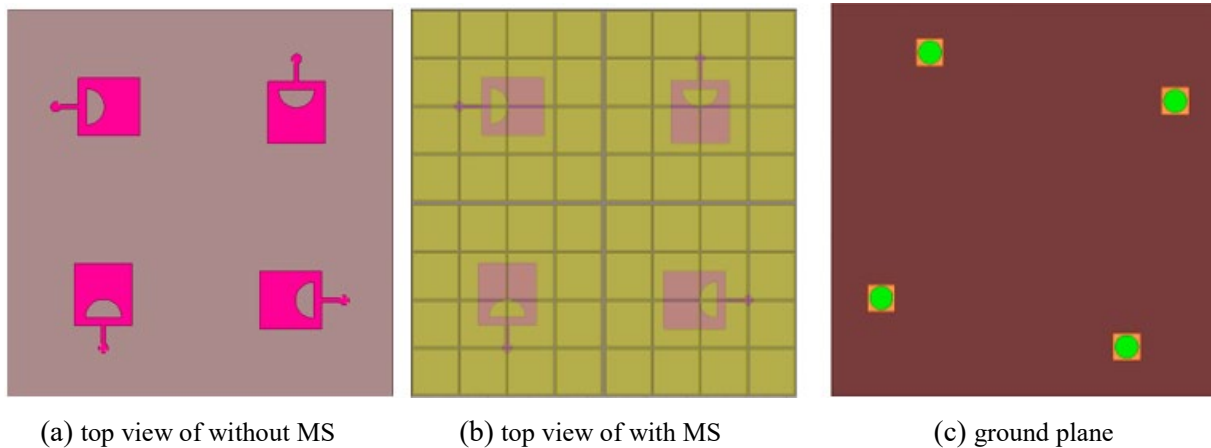


(a) top view of without MS          (b) top view of with MS          (c) ground plane

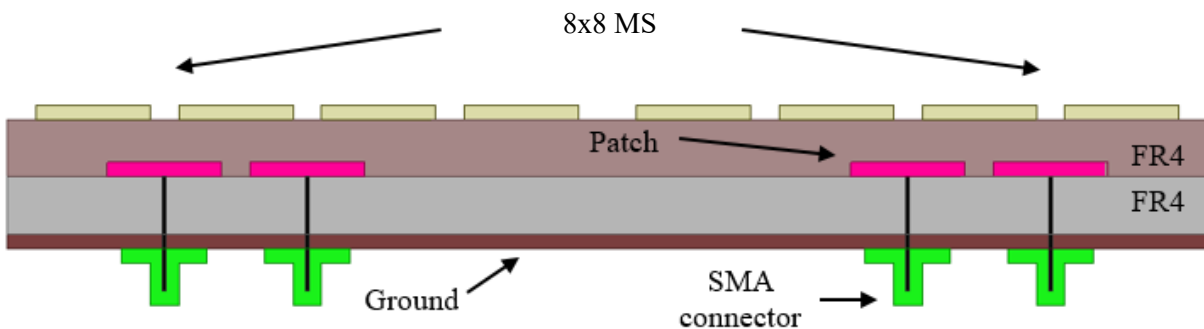**Figure 4.** The suggested MIMO antenna's geometry



**Figure 5.** Side view of suggested MIMO antenna with MS

The recommended MIMO antenna with MS is shown in side view in Fig. 5. The total dimensions of the suggested antenna with MS structure are 97 × 97 × 3.2 mm³.

## 4. SIMULATION RESULTS

MS structures are characteristically capable of being transmittive at certain frequency ranges while exhibiting reflective behavior at others. Fig. 6 illustrates that the MIMO antenna without an MS does not exhibit resonance within the observed frequency range. However, when the MS is integrated with the MIMO antenna, the structure resonates within the 3.19 to 4.06 GHz frequency band.
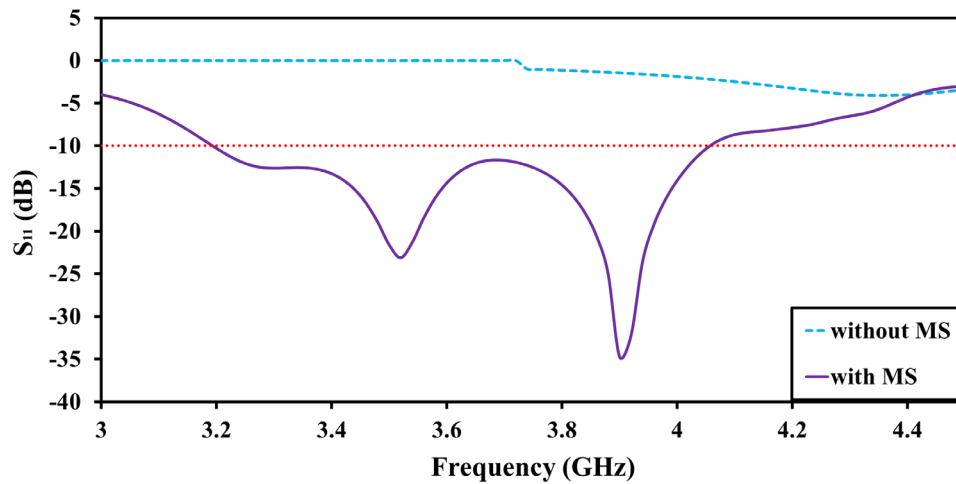


**Figure 6.** Reflection coefficient of MIMO system with and without MS
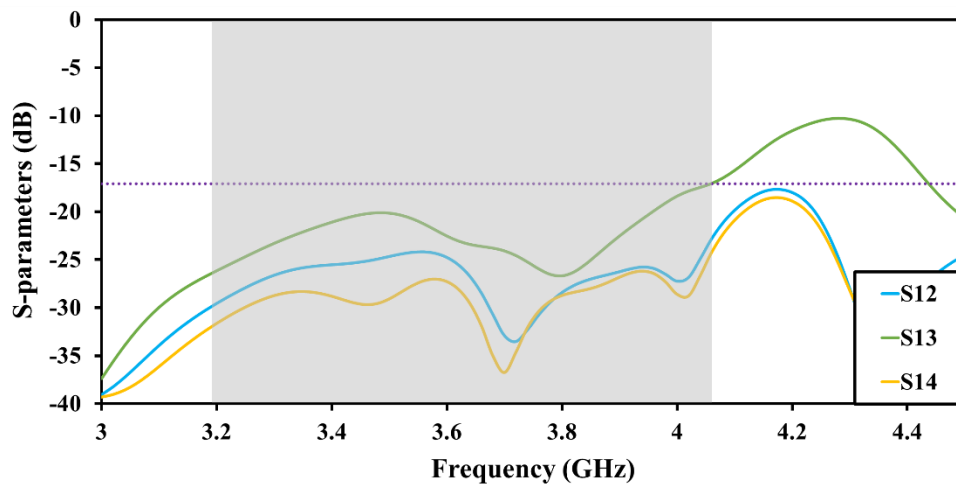


**Figure 7.** Transmission coefficient of the MIMO system with MS

Fig. 7 shows that the antenna elements have a mutual coupling of less than -17.07 dB. Gain is increased when the MS is integrated into the MIMO antenna, as in Fig. 8, with a peak gain of up to 6.85 dBi.
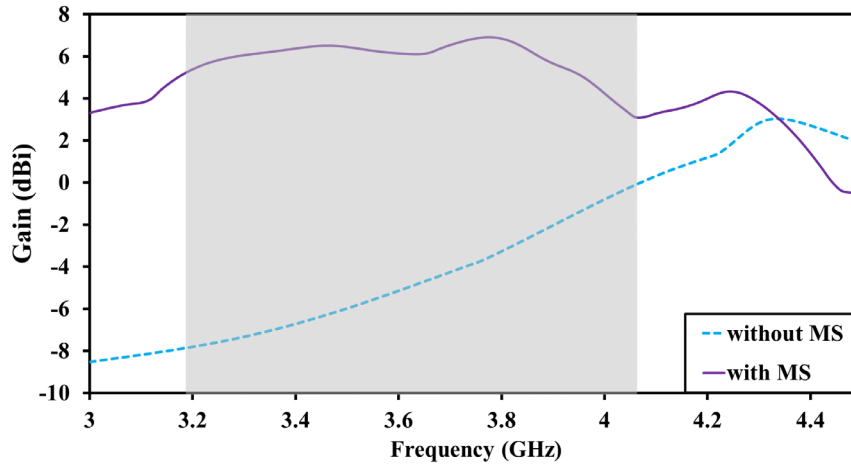
**Figure 8.** Gain of MIMO antennas with and without MS



a) 3.25 GHz, E-plane



b) 3.5 GHz, E-plane



c) 3.75 GHz, E-plane



d) 3.25 GHz, H-plane



e) 3.5 GHz, H-plane
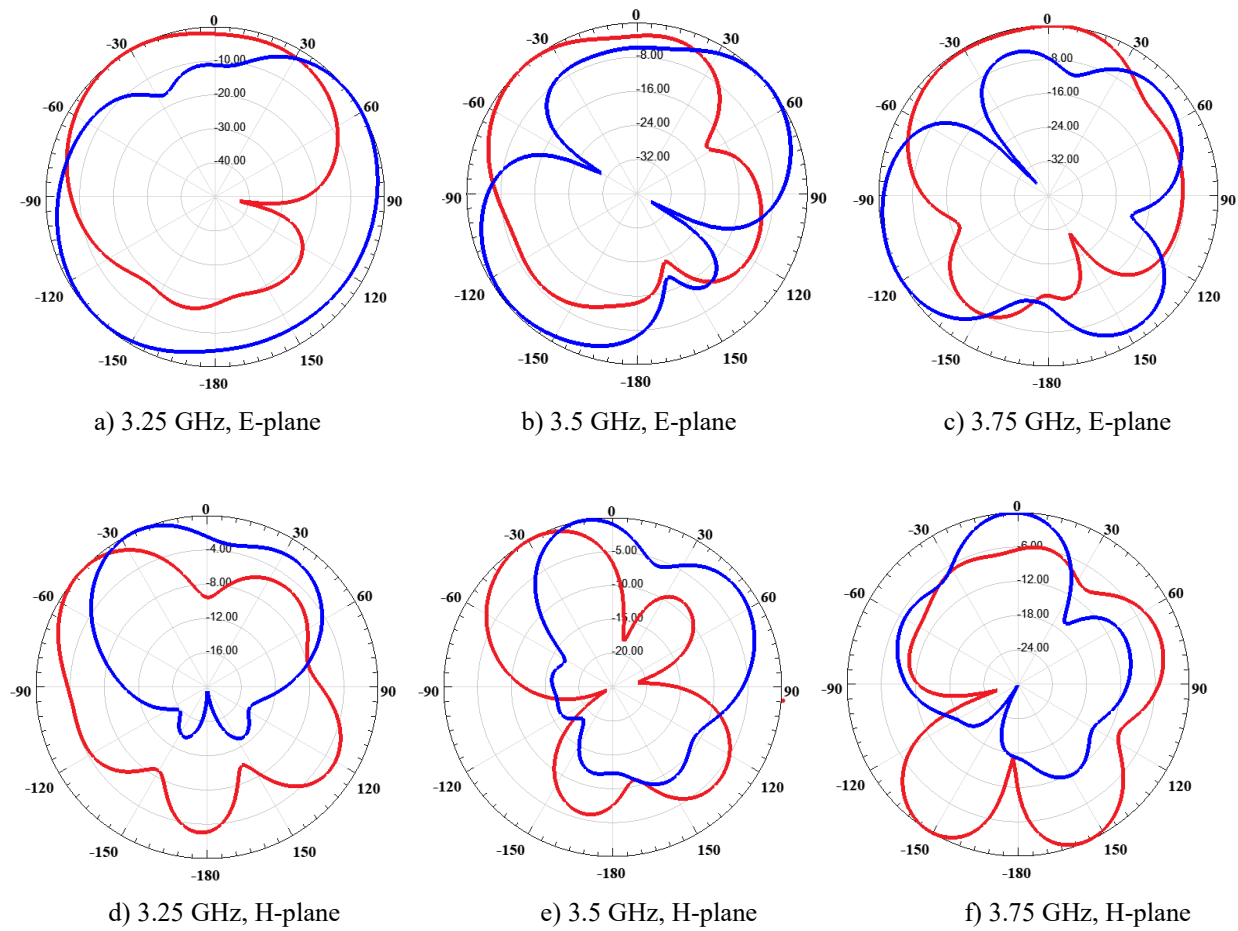


f) 3.75 GHz, H-plane

**Figure 9.** Normalized radiation patterns of the proposed MIMO antenna (red line: co-pol, blue line: cross-pol)

The images provided in Fig. 9 display normalized radiation patterns for an MIMO antenna at different frequencies and in different planes. Each plot shows co-polarization (red line) and cross-polarization (blue line). As the frequency increases from 3.25 GHz to 3.75 GHz, the radiation patterns in both E-plane and H-plane tend to become more complex, exhibiting more nulls and side lobes. This is a common characteristic as the electrical size of the antenna increases with frequency. The radiation patterns remain relatively stable across the tested frequencies, indicating consistent performance within the specified range. The E-plane and H-plane patterns exhibit typical directional characteristics, with minor variations in beam width and side lobe levels.

In order to measure isolation performance and mutual coupling between MIMO antennas, one of the parameters utilized is the envelope correlation coefficient (ECC). MIMO antennas are regarded as having good isolation if their ECC value is less than 0.5. The ECC can be calculated using Eq. 6 [18].

$$ECC = \frac{(|S_{ii}S_{ji}+S_{ij}S_{jj}|^2)}{((1-|S_{ii}|^2-|S_{ij}|^2)(1-|S_{ji}|^2-|S_{jj}|^2))} \tag{6}$$

The term $S_{ij}$ denotes the elements of the S-parameter matrix, where the indices $i$ and $j$ are assigned values such as 1, 2, 3, …, depending on how many components there are in the system, and the ECC value is subsequently calculated.
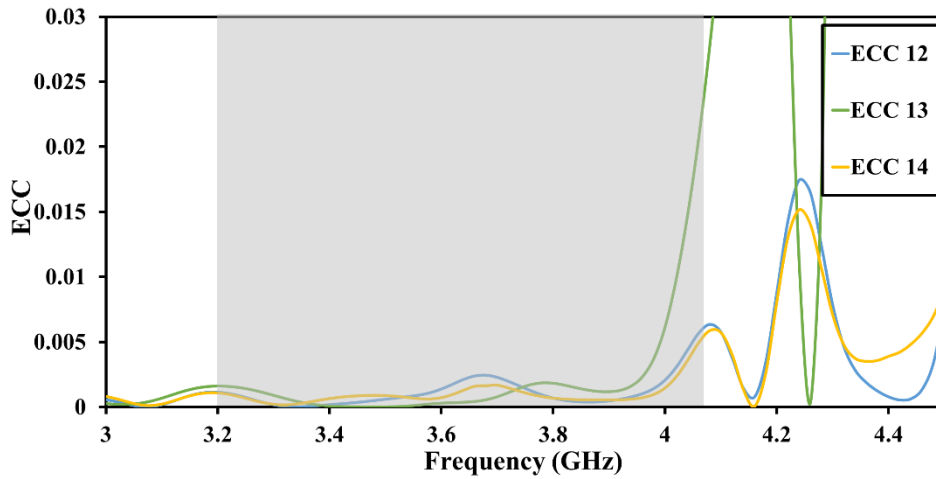
**Figure 10.** ECC values of the MS-equipped MIMO antenna

A performance parameter called diversity gain (DG) is employed in MIMO systems to lessen the impact of signal fading. The diversity gain can be calculated based on ECC, as shown in Eq. 7 [18]. Ideally, when ECC is near zero, the DG approaches 10 dB.

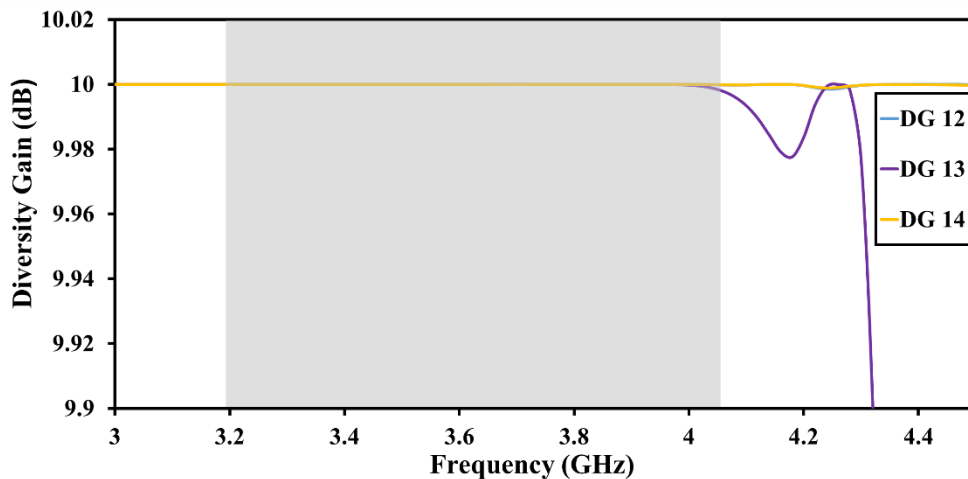$$DG_{ij} = 10\sqrt{1-\left(ECC_{ij}\right)^2} \tag{7}$$

**Figure 11.** Diversity gain of MIMO antenna with MS

The suggested MS-based MIMO antenna has a maximum ECC value of 0.02 as illustrated in Fig. 10, and as shown in Fig. 11, a DG value of 9.99 at 4.06 GHz. These findings show that the suggested MS-based MIMO antenna offers strong isolation and shows low mutual coupling among the MIMO antenna parts. A comparison of the suggested antenna and antenna designs documented in the literature is shown in Table 2. The proposed antenna exhibits the smallest dimensions in terms of λₒ among the compared designs, which provides a

significant advantage for integration into portable systems. Although Ref. [17] offers a wider bandwidth and higher peak gain, it suffers from lower isolation. Ref. [20] demonstrates a comparable bandwidth but has lower peak gain and isolation. Ref. [21] and Ref. [22] achieve higher peak gain and better isolation, yet their bandwidths are narrower. Ref. [23] and Ref. [24] exhibit lower bandwidth, peak gain, and isolation compared to the proposed antenna.

**Table 2.** Comparison of the suggested MIMO antenna's performance

| Ref. | Dimension ($\lambda_0$) | Bandwidth (GHz) | Port | Peak Gain (dBi) | Isolation (dB) |
|------|-------------------------|-----------------|------|-----------------|----------------|
| [17] | $1.1 \times 1.1 \times 0.04$ | 3.3 - 4.5 | 4 | 7.7 | >15 |
| [20] | $1.6 \times 1.6 \times 0.01$ | 3.3 - 4.2 | 4 | 4 | >10 |
| [21] | $1.62 \times 1.62 \times 0.01$ | 3.3 - 3.87 | 4 | 8.72 | >32 |
| [22] | $1.42 \times 1.42 \times 0.04$ | 3.3 - 3.91 | 4 | 13.6 | >28 |
| [23] | $1.6 \times 0.8 \times 0.017$ | 3.21 - 3.81 | 4 | 3.64 | >10 |
| [24] | $2.27 \times 1.7 \times 0.04$ | 3.4 - 3.6 | 4 | 3.5 | >11 |
| Proposed | $1.03 \times 1.03 \times 0.017$ | 3.19 – 4.06 | 4 | 6.85 | >17.07 |

## 5. CONCLUSIONS

In this study, an MS was added to a unique MIMO antenna to improve its performance, and it was examined how the MS affected different antenna characteristics. The findings unequivocally show that the MS increases the gain and allows the antenna to resonate at a certain frequency below -10 dB. The MS-based MIMO antenna, with dimensions of 1.03 λₒ × 1.03 λₒ × 0.017 λₒ, operates in the 3.19 to 4.06 GHz frequency band, thereby covering the N77 band and N78 Sub-6 GHz 5G bands. Despite the antenna elements' roughly 0.34 λₒ distance from one another, over 17 dB of inter-element isolation is achieved by the design. The proposed four-port MS-based MIMO antenna not only suits mobile communication systems but also presents an effective solution for gadgets like Internet of Things applications, smart manufacturing systems, robotic control, automation, and private 5G networks deployed in environments like airports and campuses.

## REFERENCES

[1]   Al-Dujaili MJ, Al-dulaimi MA. Fifth-generation telecommunications technologies: Features, architecture, challenges and solutions. Wireless Personal Communications. 2023;128(1):447-69

[2]   Malik BT, Khan S, Nasir J, Koziel S. Enhanced Gain and Isolation Dual-Band Dual-Port MIMO Antenna with Integrated Lens for Millimeter-wave 5G Internet-of-Things Applications. IEEE Access. 2025

[3]   Hasan MM, Islam MT, Alam T, Kirawanich P, Alamri S, Alshammari AS. Metamaterial loaded miniaturized extendable MIMO antenna with enhanced bandwidth, gain and isolation for 5G sub-6 GHz wireless communication systems. Ain Shams Engineering Journal. 2024;15(12):103058

[4]   Zhao L. A MIMO antenna decoupling network composed of inverters and coupled split ring resonators. Progress In Electromagnetics Research C. 2017;79:175-83

[5]   Tran HH, Nguyen-Trong N. Performance enhancement of MIMO patch antenna using parasitic elements. IEEE Access. 2021;9:30011-6

[6]   Khandelwal MK, Kanaujia BK, Kumar S. Defected ground structure: fundamentals, analysis, and applications in modern wireless trends. International Journal of antennas and Propagation. 2017;2017(1):2018527

[7]   Su S-W, Lee C-T, Chang F-S. Printed MIMO-antenna system using neutralization-line technique for wireless USB-dongle applications. IEEE transactions on antennas and propagation. 2011;60(2):456-63

[8]    Caloz C, Itoh T. Electromagnetic metamaterials: transmission line theory and microwave applications: John Wiley & Sons; 2005.

[9]    Yu K, Li Y, Liu X. Mutual coupling reduction of a MIMO antenna array using 3-D novel meta-material structures. Applied Computational Electromagnetics Society Journal (ACES). 2018:758-63

[10]   Zeain MY, Abu M, Althuwayb AA, Alsariera H, Al-Gburi AJA, Abdulbari AA, et al. A new technique of FSS-based novel chair-shaped compact MIMO antenna to enhance the gain for sub-6GHz 5G applications. IEEe Access. 2024

[11]   Bai H, Wang G-m, Zou X-j. A wideband and multi-mode metasurface antenna with gain enhancement. AEU-International Journal of Electronics and Communications. 2020;126:153402

[12]   Tran H-H, Nguyen TT-L, Ta H-N, Pham D-P. A metasurface-based MIMO antenna with compact, wideband, and high isolation characteristics for sub-6 GHz 5G applications. IEEE Access. 2023;11:67737-44

[13]   Ud Din I, Alibakhshikenari M, Virdee BS, Jayanthi RKR, Ullah S, Khan S, et al. Frequency-selective surface-based MIMO antenna array for 5G millimeter-wave applications. Sensors. 2023;23(15):7009

[14]   Parchin NO, Al-Yasir YIA, Ali AH, Elfergani I, Noras JM, Rodriguez J, et al. Eight-element dual-polarized MIMO slot antenna system for 5G smartphone applications. IEEE access. 2019;7:15612-22

[15]   Narayanaswamy NK, Satheesha T, Alzahrani Y, Pandey A, Dwivedi AK, Singh V, et al. Metasurface absorber for millimeter waves: a deep learning-optimized approach for enhancing the isolation of wideband dual-port MIMO antennas. Scientific Reports. 2024;14(1):1-18

[16]   Kiem NK, Phuong HNB, Chien DN. Design of compact 4× 4 UWB-MIMO antenna with WLAN band rejection. International Journal of Antennas and Propagation. 2014;2014(1):539094

[17]   Wong K-L, Ye X-Q, Li W-Y. Wideband four-port single-patch antenna based on the quasi-TM 1/2, 1/2 Mode for 5G MIMO access-point application. IEEE Access. 2022;10:9232-40

[18]   Balanis CA. Antenna theory: analysis and design: John wiley & sons; 2015.

[19]   Çelik K, Kurt E, Korkmaz O. A Novel Multiple-Slot Pixel Patch Antenna for Wideband Terahertz Applications. JOM. 2025;77(5):2967-75

[20]   Barani IRR, Wong K-L, Zhang Y-X, Li W-Y. Low-profile wideband conjoined open-slot antennas fed by grounded coplanar waveguides for 4×4 5G MIMO operation. IEEE Transactions on Antennas and Propagation. 2019;68(4):2646-57

[21]   Sufian MA, Hussain N, Askari H, Park SG, Shin KS, Kim N. Isolation enhancement of a metasurface-based MIMO antenna using slots and shorting pins. IEEe Access. 2021;9:73533-43

[22]   Da Xu K, Zhu J, Liao S, Xue Q. Wideband patch antenna using multiple parasitic patches and its array application with mutual coupling reduction. IEEE Access. 2018;6:42497-506

[23]   Rafique U, Khan S, Ahmed MM, Kiani SH, Abbas SM, Saeed SI, et al. Uni-planar MIMO antenna for sub-6 GHz 5G mobile phone applications. Applied Sciences. 2022;12(8):3746

[24]   Chen S-C, Chou L-C, Hsu C-I, Li S-M. Compact sub-6-GHz four-element MIMO slot antenna system for 5G tablet devices. IEEE Access. 2020;8:154652-62